Strojniški vestnik - Journal of Mechanical Engineering 54(2008)5, 364-371
UDC 528.02
Paper received: 20.6.2007
Paper accepted: 28.9.2007

Modern Deformation Measurement Techniques and their Comparison

Boštjan Kovačič[1,*] - Rok Kamnik[1] - Miroslav Premrov[1] - Nenad Gubeljak[2] - Jožef Predan[2] - Zdravko Tišma[2]
[1]University of Maribor, Faculty of Civil Engineering, Slovenia
[2]University of Maribor, Faculty of Mechanical Engineering, Slovenia

Deformation measurement experiment has been undertaken where a concrete structure was subject to controlled loading. Concrete plate was loaded with hydraulic cylinder PZ 100 up to 42 kN. Nikon total station ser. 720 and camera Fuji Pro S3 have been used to make measurements at critical points during each additional load. A hydraulic computer operated cylinder was used for load increase. The use of total stations for deformation measurements is quite often, but the combination with digital photography is rather new and very suitable technique. It offers the capability of simultaneous monitoring of a large number of signalized or non-signalized points with very low root mean square error of 0.16 mm in geodetic method 0.7 mm in photogrammetry, respectively. The concrete plate was modeled and the comparison with the geodetic, photogrammetric and hydraulic method was made.

Keywords: deformation measurements, geodesy, digital photogrammetry

0 INTRODUCTION

The monitoring of structures has a high importance with regard to the assessment of the reliability, availability, health diagnostics, damage detection, load rating, condition assessments, load carrying capacity estimation and model updating [1]. Control measurements can be performed in a variety of ways depending on the structures. In practice, control measurements are performed with the help of geodetic measurements, the basic goal of which is to capture any geometric changes in the measured object. Displacements and deformations are determined. This means defining the position of changes and the object's shape, with respect to the environment and time. Increasing attention to predictive maintenance and health monitoring of existing structures has prompted more and more research work back to laboratories.

Geodetic deformation measurements are quite often for such tasks [2]. Building monitoring is usually carried out with classic geodetic methods such as trigonometric heights, leveling and nowadays, also with classic or digital photogrammetry, GPS and laser scanners.

The method for fastest and easiest monitoring the points on the structure, with the very good accuracy is a trigonometric height. The step forward is to combine that method with other non-conventional methods such as photogrammetry. Photogrammetric measurement has been, till now, usually used for the needs of architecture (façade), cultural heritage (archaeological sites), medicine (face, body, skin, eyes studies etc.) and industry (quality check). With the development of accuracy in digital photography [3] it is possible to precisely monitor the deformations of objects of interest like concrete plate, bridge, building etc. [4] and [5].

This paper presents the comparison of geodetic deformation measurements with the analitical model, photogrammetric technique and the results of the vertical deflections got from the hydraulic cylinder.

1 THEORETICAL BASICS OF MEASUREMENT METHODS

1.1 Trigonometric Heights

Trigonometric height is the classic geodetic task where the altitude difference between two points is given by [6]:

$$\Delta H = S \cdot ctgZ_A + i_A - l_B + \left(\frac{1-k_a}{2}\right)\cdot\left(\frac{S^2}{R}\right) \quad (1),$$

where:

*Corr. Author's Address: University of Maribor, Faculty of Civil Engineering, Smetanova 17, SI-2000 Maribor, bostjan.kovacic@uni-mb.si

S - horizontal measured distance between A and B
Z_A - vertical distance
i_A - height of instrument at point A
l_B - height of prism at point B
k_a - coefficient of refraction (for Slovenia $k_a = 0.13$) [6]
R - Earth radius as a sphere ($R = \sqrt{M \cdot N}$; M - radius of curvature along the meridian, N - radius of curvature along the prime vertical (transverse radius of curvature); R = 6370,04 km)

In this case the height of instrument i_A can be omitted from the Eq. (1), because measurements were in a relative coordinate system and all measurement were of a fully local nature. The height of prisms l_B can also be omitted from Eq. (1), because reflective tape targets have negligible thickness.

Equation (1) can be simplified:

$$\Delta H = S \cdot ctgZ_A + \frac{S^2}{2R} - k_a \frac{S^2}{2R} \qquad (2).$$

The zenith distance can be replaced by the vertical angle (α); the refraction coefficient can be omitted (because of the laboratory conditions) so the final equation is:

$$\Delta H = S \cdot tg\alpha + \frac{S^2}{2R} - k_a \frac{S^2}{2R} \qquad (3).$$

A post-processing of all recorded data was carried out before the analysis (filtering). In this way all possible errors were eliminated, such as double observation of the same point, wrong order of sightings, etc. The observations were arranged according to individual epoch. Every load test epoch was compared with the zero state, which was recorded from the start of measurements and controlled by the control points on the wall.

The precise processing of the measured data and its analyses were performed after the field measurement. For every target the standard deviation was calculated. Ten readings were performed for each target (distance, horizontal and vertical angle) in the precise measurement mode of the instruments. The arithmetic mean values of the distance readings were calculated. For each target, the standard deviation was calculated [7]:

$$s = \sqrt{\frac{\sum v^2}{(n-1)}} \qquad (4),$$

where:
s - standard deviation,
v^2 - squared deviation from arithmetic mean
n - number of observations.

A measurement precision in distance of ± 0.16 mm, horizontal angle of ± 3.0'', vertical angle of ± 3.4'', Y coordinate of 0.13 mm, X coordinate of 0.13 mm and of Z coordinate of 0.11 mm was achieved.

This method is very fast and accurate with option of getting some of the results already on the field. To get a strong reflected signal small in incident angles should be avoided. Distance measurement represents the essential component of instrument accuracy [8].

The costs of this method increases with the number of surveyed spots. On the field, we usually must use prisms instead of tape targets (there is high installation expense).

1.2 Photogrammetric Method

Stereo-photogrammetry is an optical measuring method which has become a standard method in geodesy, civil engineering and architecture in past few decades. Measuring object is recorded using a high resolution CCD camera after which a digitalisation and computer processing of stereo-couples is made. Picture coordinates of measuring points are being searched with numerical procedures and then calculated in 3D object coordinates using a principle of triangulation. This method is suitable for accurate measuring of the position in space, three-dimensional displacement and with high number of points even measuring of object shape and deformation.

For performing a measurement, two sets of coordinates have to be defined – object (space) coordinates, which are bound to outer coordinate system and picture coordinates which define a position of measuring points on film plane and are bound to camera coordinate system. Dependency between these two coordinate sets with respect to measuring object is shown in Figure 1.

Determination of dependency between object coordinates and picture coordinates of an arbitrary point P begins with setting up a coordinate system in projective center of camera objective O (X_0, Y_0, Z_0) so that its X* and Y* axis are parallel to camera axis x and y. Z* axis is opposite to the optical axis H-O. Object coordinates of point P in this coordinate system are calculated with transformation matrix, whose elements are transformation coefficients based on angles

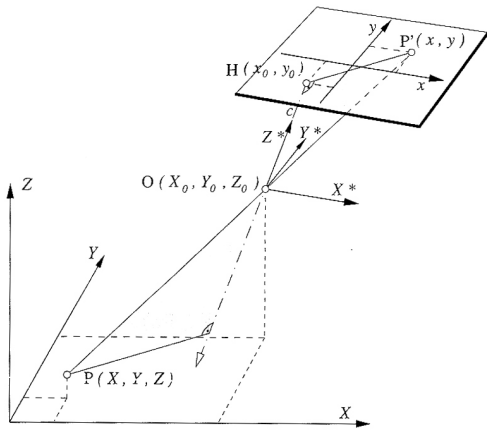

Fig. 1. *Dependency between two coordinate sets*

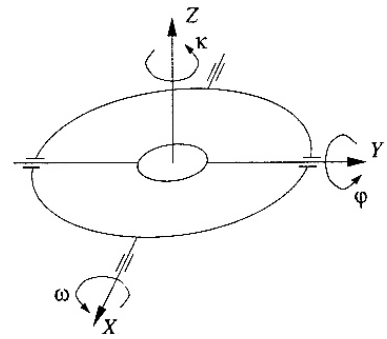

Fig. 2. *Three angles of rotation (ω, φ, κ)*

between coordinate axis. Rotation around coordinate system can be described with three independent angles of rotation (ω, φ, κ) around coordinate axis (X, Y, Z) – Figure 2.

The relation between picture coordinates (x, y) and transformed object coordinates comes from co-linearity condition [8]:

$$\begin{bmatrix} x \\ y \end{bmatrix} = \begin{bmatrix} x_O \\ y_O \end{bmatrix} - \frac{c}{Z_P^*} \begin{bmatrix} X_P^* \\ Y_P^* \end{bmatrix} + \begin{bmatrix} \Delta x \\ \Delta y \end{bmatrix} \quad (5),$$

where x_0, y_0 denotes main point's picture coordinates of snap-shot H and $\Delta x, \Delta y$ denotes deviation from central projection as a consequence of objective distortion. In general the picture coordinates can be written as:

$$\begin{aligned} x &= f\left(c, X_O, Y_O, Z_O, \omega, \varphi, \kappa, X, Y, Z, x_O, \Delta x\right) \\ y &= f\left(c, X_O, Y_O, Z_O, \omega, \varphi, \kappa, X, Y, Z, y_O, \Delta y\right) \end{aligned} \quad (6).$$

It follows that the picture coordinates are a function of six parameters of external orientation – projection center coordinates O (X_0, Y_0, Z_0) and rotation angles (ω, φ, κ) – and three parameters of internal orientation – camera constant c and picture coordinates of snap-shot's main point H (x_0, y_0). Thus if external and internal orientation of camera is known we can calculate a picture coordinate x, y for every object point.

The problems appear, if we would like to calculate object coordinates from picture coordinates. Three unknown object coordinates X, Y, Z can be calculated from two measured picture coordinates only taking extra presumption like observing a flat object which is perpendicular to recording direction so that Z coordinate is constant and known for all measuring points. For object measuring in space it is necessary to take at least one more snap-shot from different angle so that for every measuring point three or more picture coordinates can be measured. For this purpose the stereoscopic effect and method of triangulation is being used.

This principle has been used from the very beginning of stereo-photogrammetry when the measuring object was recorded with cameras from multiple positions after which the pictures (stereocouples) were being processed by using special devices called stereocomparators. Object (space) coordinates of measuring points were determined directly by using so called opto-mechanical reconstruction procedure.

In today's stereophotogrammetric measurement, an automatic – analytical procedure is being used. On stereocouples, which are recorded with CCD cameras, picture coordinates of measuring points are measured with software and for every picture coordinate one equation can be set. Provided that the number of measuring points (and by that the number of extra equation) is bigger than the number of total unknown camera parameters the system of equation becomes overdefined. Thus an exact solution doesn't exist but it needs to be found with a method of minimum deviation.

In classic stereophotogrammetry the measuring points are defined with the help of known details on measuring object or by measuring marks. If measuring marks are well recorded, the accuracy of the method is very high. For measuring position in space, movement tracking, deflection measurement and in application where high point density is not necessary the stereophotgrametric method is the most powerfull among optical methods.

Photogrammetry offers the advantages of a versatile and efficient full field three-dimensional measurement technique, offering a high precision potential at reasonable cost [9].

1.3 Hydraulic Method

There was 14 epochs where the load increased for 3 kN at a time. Each epoch was held for 400 s (static load) for measurement to be made and in the next 100 s the hydraulic cylinder PZ 100 increased the load for 3 kN. The hydraulic cylinder was controlled with a LabVIEW software. Vertical deformation, for central point 5, was measured with a very precise measuring rod attached to the main cylinder. To measure the vertical displacement, measuring rod has an electrical output with the incremental counter.

2 RESULTS

2.1 Test Configuration

In order to compare the above described measurement methods, the prefabricated prestressed concrete plate beam was made (Figure 3). Such concrete beam is frequently used for industrial buildings. Predicted vertical displacements are analytical calculated using the presented static design with the vertical force at the middle of the span. Schematic view of concrete beam is shown in Figure 4.

Deflection of the plate depends on the geometrical and material characteristics of the test sample.

Fig. 3. *Prefabricated prestressed concrete plate with measured marks*

Geometrical characteristics:
Calculated static length: *L = 3750 mm*
Width: *b = 500 mm*
Height: *h = 150 mm*
Effective depth of a cross-section: *d = 120 mm*
Cross sectional area of tensile reinforcement:
A_{s1}^{+} = 7.70 cm² (5∅14)
A_{s2}^{+} = 0.724 cm² (3×3∅3.2)
Cross sectional area of compressive reinforcement:
A_{s}^{-} = 3.93 cm² (5∅10)

Material characteristics:
Concrete:
Strength class: *C 30/37*
Mean tensile strength: $f_{ctm} = 2.9$ *MPa*
Secant modulus of elasticity: E_{cm}*=32* GPa
Mean shear modulus: G_{cm}
Reinforcement:
Strength class: *S 400* (A_{s1}^{+}, A_{s}^{-}*), S 1680* (A_{s2}^{+}*)*
Characteristic yield strength: $f_{yk} = 400$ *MPa*
Design value of modulus of elasticity:
E_s*=200* GPa

2.2 Analytical Results

The well known analytical methods can be used for calculation of non-cracked cross-section displacements. Further problems are encountered at cracked cross-sections where cracks occur in the tensile area due to the low tensile strength of a concrete. This results in reduction of the second moment of area of concrete section and consequently in deflection increasing. As it is difficult to exactly determine the location as well as the size of the cracks they are usually approximately stated using different national codes. Recently Eurocode 2 [11] has been most frequently applied in Europe and therefore considered in our analysis.

According to the presented characteristics the second moment of area of the un-cracked cross-section is $I_y^{(I)}$*=15345.478 cm⁴*.

The bending moment forming the first crack in the tensile concrete section ($M_y^{(I)}$) is calculated in the form of:

$$M_y^{(I)} = f_{ctm} \cdot \frac{2 \cdot I_y^{(I)}}{h} = 5.9336 \text{ kNm} \qquad (7).$$

For the un-cracked cross-section (M_{y0} *d"* $M_y^{(I)}$) the maximum vertical displacement (w_{inst}) is the sum of bending moment (M_{y0}), shear force (V_{z0})

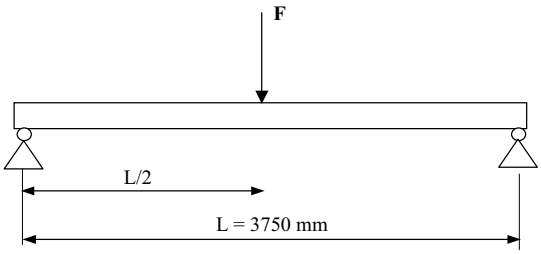

Fig. 4. *Static design of the test sample*

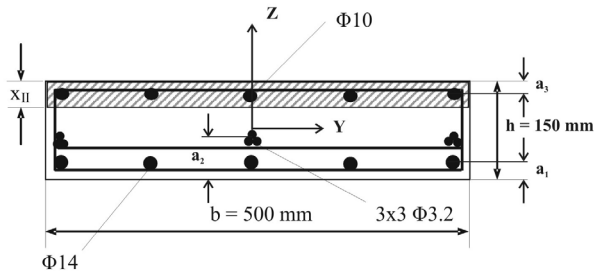

Fig. 5. *Considered elements for the cracked cross section*

and contribution (N_0):

$$w_{init} = w_{init,M} + w_{init,V} + w_{init,N} = \\ = \int_S \frac{M_{y0}(x) \cdot M_{y1}(x)}{E_{cm} \cdot I_{y,eff}^{(II)}} dx + \int_S \frac{V_{z0}(x) \cdot V_{z1}(x)}{G_{cm} \cdot A_{cs,eff}^{(II)}} dx + \int_S \frac{N_0(x) \cdot N_1(x)}{E_{cm} \cdot A_{c,eff}^{(II)}} dx \quad (8),$$

where:

A_c - cross-section area

For the treated static design (Fig. 2) Eq. (1) results in:

$$w_{init} = \frac{F \cdot L^3}{48 \cdot E_{cm} \cdot I_{yI}} + \frac{1.2 \cdot F \cdot L}{4 \cdot G_{cm} \cdot A_{cs}} \quad (9),$$

where $G_{cm} = E_{cm} / 2 \cdot (1 + \nu_c)$, $A_{cs} = A_c / 1.2$ and ν_c Poisson concrete coefficient, for which it was taken $\nu_c = 0.2$.

For the cracked cross-section ($M_{y0} > M_y^{(I)}$) the maximum vertical displacement (w_{inst}) is calculated in the form of:

$$w_{init} = w_{init,M} + w_{init,V} + w_{init,N} = \\ = \int_S \frac{M_{y0}(x) \cdot \bar{M}_{y1}(x)}{E_{cm} \cdot I_y^{(I)}} dx + \int_S \frac{V_{z0}(x) \cdot \bar{V}_{z1}(x)}{G_{cm} \cdot A_{cs}} dx + \int_S \frac{N_0(x) \cdot \bar{N}_1(x)}{E_{cm} \cdot A_c} dx \quad (10),$$

where $A_{cs,eff}^{(II)} = bx_{II} / 1.2$ and $A_{c,eff}^{(II)} = bx_{II}$.

The effective second moment of area of the cracked cross-section ($I_{y,eff}^{(II)}$) is determinated according to *Eurocode 2* in the form of:

$$I_{y,eff}^{(II)} = \xi \cdot I_y^{(II)} + (1 - \xi) \cdot I_y^{(I)}$$

$$\xi = 1 - \beta_1 \cdot \beta_2 \cdot \left(\frac{M_{yI}}{M_{y0,max}}\right)^2 \quad (11).$$

$$M_{y0,max} = \frac{F \cdot L}{4}; \quad \beta_1 = 1.0, \ \beta_2 = 1.0$$

The value of $I_y^{(II)}$ is calculated according to the neutral axis position (x_{II}) using the scheme from Figure 5 and $n = E_s / E_{cm}$:

$$\frac{b \cdot x_{II}^2}{4} + (n-1) \cdot A_s^- \cdot (x_{II} - a_3) - \\ - n \cdot A_{s1}^+ \cdot (h - a_1 - x_{II}) - n \cdot A_{s2}^+ \cdot (h - a_2 - x_{II}) = 0$$

$$x_{II} = 4.948 cm \quad (12).$$

$$I_y^{(II)} = \frac{b \cdot x_{II}^3}{3} + (n-1) \cdot A_s^- \cdot (x_{II} - a_3)^2 + n \cdot A_{s1}^+ \cdot (h - a_1 - x_{II})^2 + \\ + n \cdot A_{s2}^+ \cdot (h - a_2 - x_{II})^2 = 4757.344 cm^4$$

2.3 Measured Results Using Different Methods

For characteristic point observations trigonometric height was used. Measurements were performed from one station point (stabilised one day in advance). The measurements were made from tripod that was glued to the ground. Between each load phase a station point position was checked for stability (measurements of control points on the wall). Potential shifts of the instrument didn't occur. Before measurement the instrument was calibrated and data about air temperature and pressure were entered (both were stable during the test). First, the zero state was recorded and then one individual phase after another. Nikon series 800 instrument and precise measurement mode (PMRS) was used for the trigonometric heighting.

210 sight points on the concrete plate were observed in a local (object) coordinate system. Each point was observed with 10 iterations. Leica's reflective tape targets of dimensions 1 x 1 cm were used on each target point. In Figure 6 reflective tape targets 4, 5 and 6 in the middle of the concrete plate (where the breakage was expected) are shown.

Reference points (targets) have been used in vicinity of Leica reflective tape targets so that the deflection has been measured in the same position with both methods. A reference point is represented as a white circle of 18 mm diameter on black surface. For determination of camera position and position of reference points, the coded marks have been used. Each of them had a 15-bit type code presented by circle sectors which identifies them in every snap-shot. The correct distance between measuring points is determined

with scale bars whose distance is known and doesn't change during the measurement.

For presented measurement a stereo-photogrammetry system TRITOP was used (manufacturer GOM mbH, Braunschweig, Germany) with high resolution CCD camera Fuji Pro S3 (4256 x 2848 pixels) and software for calculation and analysis of object coordinates (Fig. 5). In each loading stage minimum 8 snap-shots from different angles and position were made so that all the points were visible. Camera positions were not stabilized. Snap-shots of each loading stage have been processed during the measurement so that the deflections from previous stages were already known. Maximum standard deviation of measuring results was 0.08 mm.

2.4 Comparison of Results

A comparison of the calculated analytical and (measured) geodetic, (measured) photogrammetric vertical displacements and (measured) hydraulic cylinder vertical displacements was made. Table 2 shows vertical displacements by epochs for point 5 in the middle of the concrete plate (because only point 5 was monitored with all three methods). In practice there is an unwritten rule that the ratio between calculated and measured value should not be less then 75 %. We neglected the first two epochs that the mean ratio between calculated and measured values was 88.5 %.

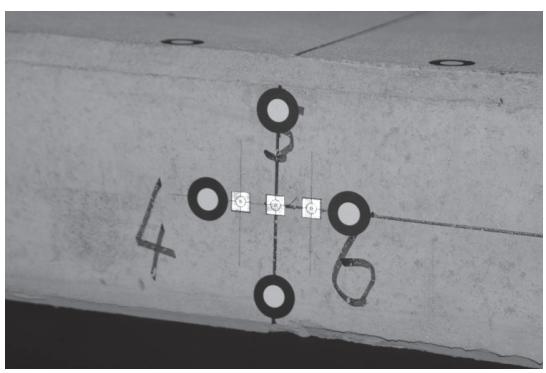

Fig. 6. *Reflective tape targets 4, 5 and 6 in the middle of the concrete plate*

The comparison of measurements of vertical displacements for the whole concrete plate was made. The geodetic and photogrammetric results were comparable (some tenth of mm) for point 5 (Fig. 8). It can be seen that the surveyed vertical displacement was always smaller then the calculated values. There is a small deviation in the first two epochs because of local contact surface under hydraulic piston was undefined.

3 CONCLUSION

Load deformation of a concrete plate can be monitored with a variety of different methods. We can choose the method by a construction dimensions, presumed displacements, access to the construction and also field and weather conditions. In practice, it is reasonable to use at least two independent methods for pretentious constructions. In that way we increase cost and duration of measurements but on the other hand we can get more trustworthy and non uniform results. If we measure more data that is needed for uniform results, we can make all sorts of statistical analyses at the time of data processing.

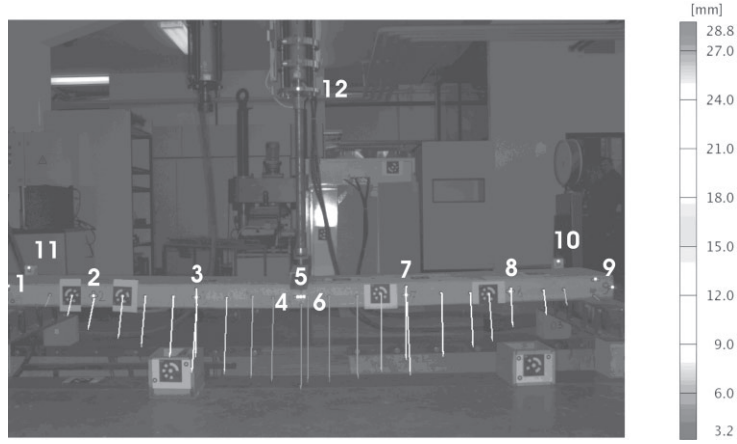

Fig. 7. *Reference points, coded marks, scale bars and displacement vectors of a concrete plate*

Table 1. *Vertical displacement by epochs for point 5 in the middle of the concrete plate*

[kN]	Point	Vertical displacement			
		Analytical	Hydraulic	Photo	Geodetic
3	5	-0.7	-1.5	-0.9	-1.0
6	5	-1.3	-2.3	-1.8	-1.8
9	5	-6.4	-4.1	-3.5	-3.6
12	5	-8.6	-6.0	-6.7	-6.9
15	5	-10.8	-9.2	-8.6	-8.7
18	5	-13.0	-11.6	-11.4	-11.6
21	5	-15.2	-14.1	-13.8	-14.0
24	5	-17.3	-16.7	-16.4	-16.4
27	5	-19.5	-18.7	-18.2	-18.4
30	5	-21.7	-21.6	-21.2	-21.3
33	5	-23.9	-23.4	-22.4	-22.8
36	5	-26.1	-25.6	-24.6	-25.2
39	5	-28.2	-27.8	-26.6	-27.1
42	5	-30.4	-30.1	-28.7	-29.1
Average ratia analitycal/ measured			90.5 %	86.8 %	88.2 %

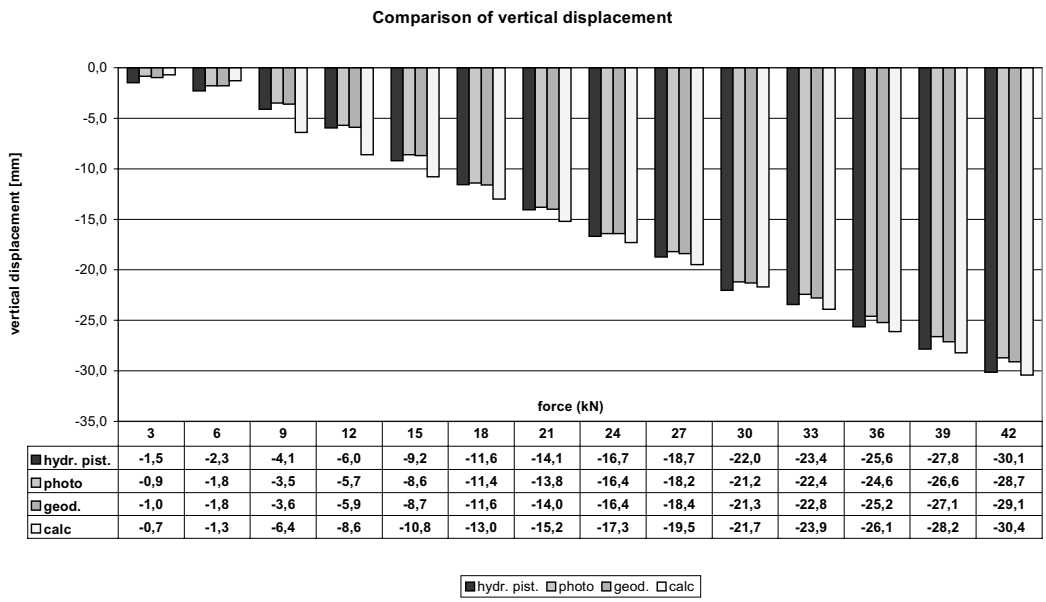

Fig. 8. *Comparison of vertical displacement in point 5*

In our case we used four independent methods. Three measurement methods and one analytical. The goal of all measurements was comparison of methods and find out which method is most comparable with calculated results. One of goals was also to test photogrammetric results which are rather new for that kind of testing in Slovenia. The results are showing that al methods are suitable and accurate what can be seen in *Table 1* and *Figure 8*. The results show that the agreement between hydraulic piston and analytical calculation was 90 %, photogrammetric 86 % and geodetic 88 %. In practice the agreement is usually taken over 75 %. Closer look at the results shows, that we used too few photogrammetric measurements, geodetic method is very sensitive to outer conditions meanwhile hydraulic piston is most accurate with 1/100 mm but suitable only for indoor laboratory testing. In field, there is a good combination of photogrammetric and geodetic methods but only if the access and the construction is suitable. The problem with access is in the case of bridges where water prevents to take photos from the middle of the

span, meanwhile geodetically we can measure even those points.

From results we can conclude that we got very good accuracy with comparison of results, so in practice we can use each one.

We will continue with our tests and compare these methods with other. Further research will be on the field of redundant measurement analyses, motorized geodetic measurements and better algorithms for calibration, snap-shot processing and the calculation of three-dimensional coordinates, which, in combination with development of new cameras, will lead to even better accuracy and use of the method.

4 REFERENCES

[1] Ataei, S., et al. Sensor fusion of a railway bridge load test using neural networks. *Expert Systems with Applications*, 29, 2005, p. 678-683.

[2] Kovačič, B., Kamnik, R. Measurement of displacement and deformations on the biggest Slovenian viaduct, with particular stress on accuracy calculations. *Allgemaine Vermessungs Nachrichten*, 10/2006, p. 322-328.

[3] Dörstel, C., Jacobsen K., Stallmann D. DMC - Photogrammetric accuracy - Calibration aspects and generation of synthetic DMC images. *Proceedings of Optical 3D Measurements Symposium*, Zürich, 2003.

[4] Albert, J., Maas H.G., Schade, A., Schwarz W. Pilot studies on photogrammetric bridge deformation measurement. *IAG Berlin, Proceeding of the 2nd Symposium on Geodesy for Geotechnical and Structural Engineering*, Berlin, Germany, May 21-24, 2002.

[5] Gordon, S., et. al. Measurement of structural deformation using terrestrial laser scanners. *1st FIG International Symposium on Engineering Surveys for Construction Works and Structural Engineering*, Nothingham, UK, 28. junij - 1. julij, 2004.

[6] Vodopivec, F. *Trigonometric heights*. Department of civil engineering and Department of geodesy FAGG. University of Ljubljana, 1985. (In Slovenian)

[7] Moseru, A., *Ingeneering geodesy, Basics.* 3rd Ed. Heidelberg: Wichmann, Germany, 2000. (In German)

[8] Wunderlich, T. A. Geodetic monitoring with prismless polar methods. *INGEO 2004 and FIG Regional Central and Eastern European Conference on Engineering Surveying*, Bratislava, Slovakia, November 11-13, 2004.

[9] Gorjup, Z. *Photogrammetric basis.* University of Ljubljana, FGG, Ljubljana, 2001. (In Slovenian)

[10] Maas, H.G., Hampel, U. Photogrammetric tehniques in civil engineering material testing and structure monitoring. *Photogrammetric Sensing & Remote Sensing*, vol. 72, no. 1, 2006.

[11] *CEN, Eurocode 2: Design of concrete structures – Part 1: General rules and rules for buildings*, 2002.